Biomimetic Synthesis of Titanium Dioxide Utilizing the R5 Peptide Derived from *Cylindrotheca fusiformis*

Sarah L. Sewell and David W. Wright*

Department of Chemistry, Station B 351822, Vanderbilt University, Nashville, Tennessee 37535

Received February 10, 2006. Revised Manuscript Received April 19, 2006

Current approaches to the synthesis of metal oxides generally require harsh conditions. In contrast, many biological processes can produce intricate metal oxide nanostructures under ambient conditions. For example, the diatom *Cylindrotheca fusiformis* forms reproducible nanostructures from silicic acid using species specific peptides known as silaffins. Herein, we report that the R5 peptide a bioinspired analogue derived from the NatSil protein in *C. fusiformis* can form titanium dioxide (TiO_2) in a concentration dependent manner from the non-natural substrate, titanium bis(ammonium lactato)-dihydroxide. Additionally, the polypeptide poly(L-lysine) acts as a template for the biomimetic synthesis of TiO_2. Subsequently, the nanoparticles were characterized using scanning electron microscopy, energy-dispersive X-ray spectrometry, and IR spectroscopy. A variable temperature X-ray diffraction study of the titanium dioxide phase transition from anatase to rutile was conducted. A delay in transition temperature was observed with titanium dioxide synthesized in the presence of phosphate buffer.

Introduction

The chemical synthesis of many metal oxides often requires extremes of temperature and pressure.[1,2] In contrast, many biological systems process metal ions under benign reaction conditions in aqueous solutions.[3] For example, magnetotactic bacteria produce iron oxide nanoparticles, which help direct them by alignment with the earth's magnetic field.[4] Ferritin, a 450 kD protein, serves as an iron oxyhydroxide storage unit in mammals.[5] By mimicking the chemistry of these natural processes, the constrained environment of ferritin has been used to form non-natural oxohydroxides of cobalt, manganese, and nickel under ambient conditions.[6−8] The metal oxide synthesis mediated by silicatein is another example of natural templates forming non-natural metal oxides. Morse and co-workers have investigated the in vitro activity of silicateins, isolated from sponge spicules, in catalyzing the enzymatic formation of silica, titanium dioxide, and gallium oxide.[9−11] This suggests that biological systems may be harnessed to expand their natural repertoire of substrates to form non-natural metal oxides.

In addition to silicatein, the in vitro silica precipitating ability of peptides derived from the diatom *Cylindrotheca fusiformis* has been extensively studied.[12] Structural studies of one such peptide, NatSil1A, revealed that the serine residues were phosphorylated resulting in a self-assembled structure containing approximately 700 peptide molecules.[13] Additionally, post-translational modification of the peptide's lysines formed ϵ-*N*-dimethyl-lysine, ϵ-*N*-trimethyl-δ-hydroxylysine, and long chain polyamines, derivatives of polypropylenimine.[14] The silica precipitating activity of the R5 peptide (SSKKSGSYSGSKGSKRRIL), a biomimetic analogue derived from a repeat unit of the NatSil gene, has also been investigated.[15] Mutation studies by Knecht and Wright have shown that the R5 peptide self-assembles to produce silica, and the RRIL motif is critical for the supramolecular self-assembled structure of this peptide.[16] Diatoms also contain long chain polyamines such as *N*-methylated poly(propylene imines) attached to putrescine cores that are capable of precipitating silica.[14] Patwardan and co-workers have investigated the ability of poly(L-lysine) (PLL), as well as a variety of other cationic polymers such as poly(L-histidine) and poly(L-arginine), to form silica from

* To whom correspondence should be addressed. E-mail: david.wright@vanderbilt.edu. Phone: (615) 322-2636. Fax: (615) 343-1234.

(1) Rao, C. N. R., Raveau, B., Eds. *Transition Metal Oxides: Structure, Properties, and Synthesis of Ceramic Oxides*, 2nd ed.; Wiley: New York, 1998.
(2) Koch, C. C. *Nanostructured Materials*; William Andrew: Norwich, 2002.
(3) Slocik, J. M.; Knecht, M. R.; Wright, D. W. In *Encylopedia of Nanoscience and Nanotechnology*; Nalwa, H. S., Ed., 2004; Vol. 1, pp 293−308.
(4) Blackmore, R. *Science* **1975**, *190*, 377−379.
(5) Harrison, P. M.; Treffry, A.; Lilley, T. H. *J. Inorg. Biochem.* **1986**, *27*, 287−293.
(6) Douglas, T.; Stark, V. T. *Inorg. Chem.* **2000**, *39*, 1828−1830.
(7) Okuda, M.; Iwahori, K.; Yamashita, I.; Yoshimura, H. *Biotechnol. Bioeng.* **2003**, *84*, 187−194.
(8) Hosein, H.-A.; Strongin, D. R.; Allen, M.; Douglas, T. *Langmuir* **2004**, *20*, 10283−10287.
(9) Cha, J. N.; Shimizu, K.; Zhou, Y.; Christiansen, S. C.; Chemelka, B. F.; Stucky, G. D.; Morse, D. E. *Proc. Natl. Acad. Sci. U.S.A.* **1999**, *96*, 361−365.
(10) Sumerel, J. L.; Yang, W.; Kisailus, D.; Weaver, J. C.; Choi, J. H.; Morse, D. E. *Chem. Mater.* **2003**, *12*, 4804−4809.
(11) Kisailus, D.; Choi, J. H.; Weaver, J. C.; Yang, W.; Morse, D. E. *Adv. Mater.* **2005**, *17*, 314−318.
(12) Kroger, N.; Deutzmann, R.; Sumper, M. *J. Biol. Chem.* **2001**, *276*, 26066−26070.
(13) Kroger, N.; Lorenz, S.; Brunner, E.; Sumper, M. *Science* **2002**, *298*, 584−586.
(14) Kroger, N.; Deutzmann, R.; Bergsdorf, C.; Sumper, M. *Proc. Natl. Acad. Sci. U.S.A.* **2000**, *97*, 14133−14138.
(15) Kroger, N.; Deutzmann, R.; Sumper, M. *Science* **1999**, *286*, 1129−1132.
(16) Knecht, M. R.; Wright, D. W. *Chem. Commun.* **2003**, *24*, 3038−3039.

10.1021/cm060342p CCC: $33.50
Published on Web 05/28/2006

silicic acid in vitro.[17−21] In the presence of PLL, metal oxides such as germanium oxide have been formed, demonstrating that the mechanism of PLL metal oxide formation can be expanded to include non-natural substrates.[22]

Increasingly, biomimetic approaches are being applied to the synthesis of a wide variety of abiological materials.[7,8,10,11,22−25] Recently, Pender and co-workers have shown that a multifunctional peptide with an R5 module can be used to mediate the formation of carbon nanotube/metal oxide (SiO_2 and TiO_2) composite materials.[26] This study did not examine, in detail, the reactivity of the R5 module toward TiO_2 formation, undoubtedly because of the complex nature of the heterogeneous conditions at which the work was performed. In contrast to the heterogeneous conditions of Pender et al. or the typical high temperatures, pressures, and caustic chemicals required for the chemical synthesis of titanium dioxide (TiO_2),[27−29] we report the first detailed examination of the R5 peptide and the polymer PLL to condense nanoparticles of TiO_2 from a titanium bis(ammonium lactato)dihydroxide (TBALDH, $[CH_3CH(O^-)CO_2NH_4]_2$-$Ti(OH)_2$) precursor under ambient conditions. The resulting nanoparticles were characterized by scanning electron microscopy (SEM), energy-dispersive X-ray spectrometry (EDS), Fourier transform infrared (IR) spectroscopy, and X-ray diffraction (XRD) patterns. The results presented here expand the known reactivity of this biomimetic peptide assembly and provide methods that can be readily adapted for a range of metal oxide syntheses.

Experimental Section

Peptide Synthesis. All peptides were synthesized on single substituted 2-chlorotrityl resins (Synpep and Adv. Chemtech) using an Advanced Chemtech Apex 396 DC automated peptide synthesizer. A standard 9-fluorenylmethoxycarbonyl (FMOC) and *tert*-butyl protection scheme was used.[30] All couplings were carried out with 5 equiv of excess to the resin capacity. Couplings were achieved by the addition of FMOC amino acid, 2-(1*H*-bezotriazole-1-yl)-1,1,3,3,-tetramethyluronium hexafluorophosphate (Anaspec), 1-hydroxybenzotriazole (Anaspec), and diisopropylethylamine (Adv. Chemtech; 1:1:1:2) followed by mixing for 1 h. FMOC was removed with 25% piperdine in a dimethyl formamide (v/v) solution. Peptides were cleaved in 1.5 mL of trifluoroacetic acid (TFA), anisole, thianisole, and 1,2-ethanedithiol (90:5:3:2) per 100 mg of resin and collected with cold diethyl ether precipitation followed by centrifugation and three washes of diethyl ether. The peptides were purified using reverse phase HPLC on a Waters Prep LC 4000 with water (0.1% TFA) and acetonitrile (0.1% TFA) on a Waters 25 mm module C_{18} column and a Waters 2487 Dual λ absorbance detector (210 and 254 nm). The identities of the peptides were confirmed using matrix assisted laser desorption ionization mass spectrometry with a time-of-flight detector. Purified peptides were lyophilized (Labconco Freesezone 4.5) and stored at −40 °C.

TiO_2 Precipitation Assay. Titanium(IV) bis(ammonium lactato)-dihydroxide (20 μL, 1 M) was added to 200 μL of various concentrations of R5 peptide or PLL·HBr (average molecular weight: 55 000 g/mol) dissolved in either phosphate buffer or water and shaken for 5 min. The samples were centrifuged for 5 min at 10 000 rpm and washed three times with deionized water. To examine the effect of pH on TiO_2 formation (Supporting Information), fresh solutions, using phosphate buffers ranging from pH 5.5 to 7.5, were used. All other experiments were conducted at a pH of 7.5.

Titanium Quantitation. The 5-chlorosalicylic acid assay was used to quantitate TiO_2 production.[31] TiO_2 was dissolved in 1 mL of concentrated sulfuric acid and incubated at 95 °C for 2 h. 5-Chlorosalicylic acid (2.5 mL of 2.5% in ethanol), sodium perchlorate (2.5 mL, 1 M), ethanol (7.5 mL), and deionized water (10 mL) were added to the dissolved titanium solution. The solution was adjusted to pH 4 using concentrated NH_4OH and diluted to 50 mL using deionized water. The colorimetric product was monitored at 355 nm using an Agilent 8453 UV−vis spectrophotometer and quantitated using a standard curve.

Template Characterization. All dynamic light scattering (DLS) measurements were conducted on a Malvern Nano Series Zetasizer with a 633 nm laser. The duration of the scans was 60 s, and 10 scans were accumulated. Circular dichroism (CD) spectra were collected on an Aviv 215 CD spectrophotometer over the wavelength range of 180−230 nm with a resolution of 3 nm and a bandwidth of 1 nm. The samples were analyzed in a strain free quartz cell with a 0.5 s averaging time. For in situ experiments, 30 μL of 1 M TBALDH was added to 250 μL of 7.5 mg/mL PLL solution in either water or phosphate buffer. An average of 20 scans were taken, and phosphate and TBALDH blanks were manually subtracted from the spectra.

Nanoparticle Characterization. Powder XRD scans were obtained on a Scintag X_1 θ/θ automated powder diffractometer with a Cu target, a Peltier cooled solid-state detector, and a zero background Si(510) sample support. The step size was 0.02, and the preset time was 25 s. All samples were scanned from 20 to 60 2Θ. For high-temperature runs, the samples (15 mg) were heated in a sealed quartz tube with nitrogen flowing in a 79300 Thermolyne tube furnace. All peaks were identified according to JCPDS. For crystal size analysis, each XRD scan was corrected for background scattering and was stripped of the Kα_2 portion of the diffracted intensity using the DMSNT software (version 1.30c), provided by Scintag. Observed peaks were fitted with a profile function to extract the full width at half-maximum (fwhm) values. The average crystallite size, L, was calculated from Scherrer's equation, $L = K\lambda/(\beta \cos \theta_B)$, assuming that peak broadening arises from size effects only (where β is the peak at fwhm measured in radians on

(17) Patwardhan, S. V.; Clarson, S. J. *J. Inorg. Organomet. Polym.* **2003**, *13*, 193−203.
(18) Patwardhan, S. V.; Clarson, S. J. *J. Inorg. Organomet. Polym.* **2003**, *13*, 49−53.
(19) Patwardhan, S. V.; Mukherjee, N.; Clarson, S. J. *Silicon Chem.* **2002**, *1*, 47−55.
(20) Patwardhan, S. V.; Mukherjee, N.; Clarson, S. J. *J. Inorg. Organomet. Polym.* **2002**, *11*, 193−198.
(21) Patwardhan, S. V.; Mukherjee, N.; Clarson, S. J. *J. Inorg. Organomet. Polym.* **2002**, *11*, 117−121.
(22) Patwardhan, S. V.; Clarson, S. J. *Polymer* **2005**, *46*, 4474−4479.
(23) Allen, M.; Willits, D.; Young, M.; Douglas, T. *Inorg. Chem.* **2003**, *42*, 6300−6305.
(24) Flynn, C. E.; Mao, C.; Hayhurst, A.; Williams, J. L.; Georgiou, G.; Iverson, B.; Belcher, A. M. *J. Mater. Chem.* **2003**, *13*, 2414−2421.
(25) Dickerson, M. B.; Naik, R. R.; Stone, M. O.; Cai, Y.; Sandhage, K. H. *Chem. Commun.* **2004**, 1776−1777.
(26) Pender, M. J.; Sowards, L. A.; Hartgerink, J. D.; Stone, M. O.; Naik, R. R. *Nano Lett.* **2006**, *6*, 40−44.
(27) Wold, A. *Chem. Mater.* **1993**, *5*, 280−283.
(28) Trentler, T. J.; Denler, T. E.; Bertone, J. F.; Agrawal, A.; Colvin, V. L. *J. Am. Chem. Soc.* **1999**, *121*, 1613−1614.
(29) Mockel, H.; Giersig, M.; Willig, F. *J. Mater. Chem.* **1999**, *9*, 3051−3056.
(30) Chan, W. C., White, P. D., Eds. *Fmoc Solid Phase Peptide Synthesis*; Oxford Univeristy Press: New York, 2000.
(31) Abdel-Aziz, M. S.; Idriss, K. A.; Sedaira, H. *Analyst* **1996**, *121*, 1079−1084.

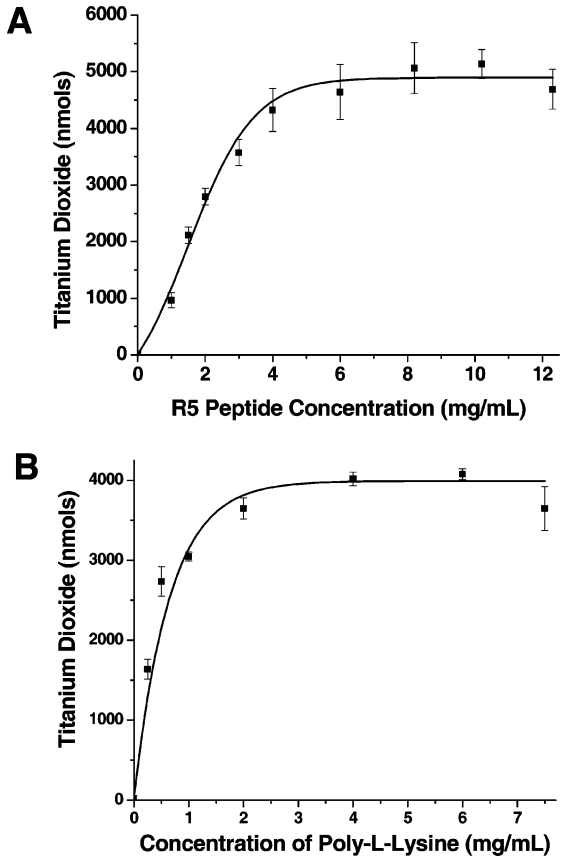

Figure 1. (A) TiO_2 produced as a function of R5 concentration. (B) TiO_2 produced as a function of PLL concentration. Reactions were run for 5 min in 100 mM phosphate buffer, pH 7.5, as detailed in the experimental section.

the 2θ scale, λ is the wavelength of X-rays used, θ_B is the Bragg angle for the measured *hkl* peak, and *K* is a constant equal to 0.90 for *L* taken as the volume-averaged crystallite dimension perpendicular to the *hkl* diffraction plane). Additionally, the nanoparticles were examined by a Hitachi S4200 scanning electron microscope operating at variable voltages. The samples were suspended in ethanol and added dropwise to an aluminum SEM puck (Ted Pella, Inc.). After evaporation of the solvent, the samples were sputter coated with a thin layer of gold (Pelco model 3 Sputtering Instrument) to avoid charging. The nanoparticles were analyzed on a Phillips CM 20T transmission electron microscope (TEM) operating at 200 kV. Samples were prepared by pipetting the nanoparticle solution on a 3 mm diameter nickel or copper grid covered with carbon film as a substrate (SPI supplies) and allowing it to evaporate. The TEM contains an EDAX DX-4 package for EDS. Samples were tilted at a 15° angle for EDS analysis.

Results and Discussion

Peptide Mediated Formation of TiO_2. The R5 peptide catalyzed the condensation of an aqueous solution of TBALDH to form amorphous TiO_2 nanoparticles at room temperature in a concentration dependent fashion (Figure 1A). As the concentration of peptide increased, the amount of TiO_2 increased linearly until approximately 6 mg/mL, where the yield approached 5000 nmols of TiO_2. In the absence of peptide, no precipitate was observed at room temperature. Previous studies, using the aqueous TBALDH precursor alone, report no formation of TiO_2 at temperatures lower than 100 °C.[29] The specific activity of the R5 peptide

Table 1. Characterization of TiO_2 Precipitating Peptides and the Resulting Nanoparticles

peptide template[a]	template size[b] (nm)	specific activity[c]	particle size (nm)
SSKKSGSYSGSKGSKRRIL	758 ± 82	2.16 ± 0.23	50 ± 20
SSKKSGSYSGSKGSKRRIL in H_2O	746 ± 150	0.75 ± 0.4	50 ± 20
SSKKSGSY	n/a	0.16 ± 0.03	n/a
SGSKGSKRRIL	637 ± 117	1.63 ± 0.09	60 ± 30
SSKKSGSYRRIL	567 ± 40	1.17 ± 0.11	50 ± 20
PLL	1570 ± 192	27.0 ± 2.0	140 ± 60
PLL in H_2O	797 ± 136	31.4 ± 5.6	40 ± 20

[a] Unless specified, reaction was performed in 100 mM phosphate buffer, pH 7.5. [b] As measured by DLS. [c] Specific activity is reported as nmoles TiO_2 per min·nmole peptide.

was 2.16 ± 0.23 nmols of titanium per min·nmol peptide, comparable to the silica specific activity of the R5 peptide reported by Knecht and Wright (Table 1),[16] with a molar ratio of titanium to R5 peptide of approximately 11. This is comparable to both the molar ratio of silica to the R5 peptide or NatSil1A, which has been reported as 13 and 12, respectively.[15,16] Approximately 20% of the available precursor was converted to TiO_2, suggesting that the precipitating TiO_2 nanoparticles may have removed the catalytic peptide from solution by encapsulation. The pH profile of TiO_2 production reached a maximum between pH 6.0 and 7.5 (Supporting Information) with well-defined nanoparticles at pH 7.5. One notable difference between the R5 mediated formation of SiO_2 and TiO_2 was that the R5 peptide exhibited TiO_2 precipitating activity in the absence of phosphate ions, albeit at reduced levels.[13,32] Given the noted similarity of the reactivity space occupied by the R5 assembly, it is likely that condensation of the TBALDH precursor occurs in a fashion similar to that of monosilicic acid. As has been suggested by several groups,[15,16] the peptide assembly can concentrate the anionic precursor through a combination of electrostatics and hydrogen bonding to promote condensation. Subsequently, the amine rich peptide template can be seen to act as a general acid/base catalyst by protonating the coordinated lactate ligand and priming the precursor for subsequent hydrolysis.

To explore the role of the R5 peptide in TiO_2 formation, a series of related peptides was examined (Table 1). While truncates SSKKSGSYRRIL (**1**) and SGSKGSKRRIL (**2**) precipitated TiO_2, the RRIL deficient truncate SSKKSGSY (**3**) was inactive. The lack of TiO_2 precipitation catalyzed by **3** suggests that the self-assembled peptide structure is vital for the production of TiO_2 in a manner similar to the R5 mediated silica results of Knecht and Wright.[16] DLS experiments of the self-assembled peptide structure reveal no self-assembly for truncates without the RRIL motif or mutations within the motif.[16] Consequently, the RRIL motif may be seen to mediate the assembly of the R5 template creating a highly cationic complex capable of interacting with multiple anionic TBALDH precursor molecules and driving subsequent condensation.

PLL has been examined as a template for the biomimetic synthesis of metal oxides including silica and germanium

(32) Sumper, M.; Kroger, N. *J. Mater. Chem.* **2004**, *14*, 2059−2065.

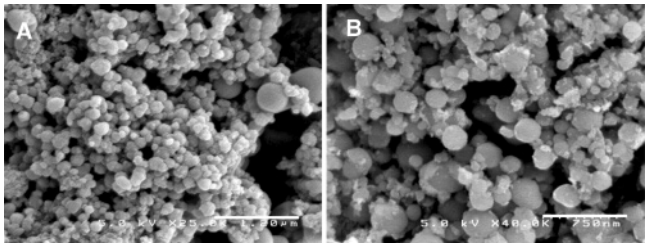

Figure 2. (A) SEM micrograph of R5 templated TiO_2 nanoparticles (scale bar 1.20 μm). (B) SEM micrograph of PLL templated TiO_2 nanoparticles (scale bar, 750 nm). Particles were obtained by reacting 20 μL of 1 M TBALDH with 200 μL of 2 mM R5 or PLL dissolved in 100 mM phosphate buffer, pH 7.5.

oxide.[20,22,33] When TBALDH was added to variable concentrations of PLL in either phosphate buffer or water, a white precipitate formed rapidly. No precipitate was observed in the absence of polymer. As the concentration of PLL increased up to approximately 2 mg/mL, the amount of TiO_2 produced increased linearly until production plateaued near 4000 nmols of TiO_2 (Figure 1B). The specific activity of PLL is 27.0 $\pm$ 2.0 nmols of titanium per min·nmol peptide (Table 1). However, when the specific activity of the R5 peptide and PLL is normalized to the number of primary amines available, it is roughly equivalent. During the course of the reaction, 20% of the starting material formed TiO_2. Analogous to the R5 mediated TiO_2 formation, TiO_2 is also formed when phosphate ions are absent. DLS studies show that the polymer approximates the size of the self-assembled structure of the R5 peptide. The reactivity and self-assembled nature of the PLL template and the R5 peptide suggest that the mechanisms of metal oxide formation are similar.[22,34,35]

Nanoparticle Characterization. SEM images of R5 peptide templated TiO_2 showed a Gaussian size distribution with a mean of 50 $\pm$ 20 nm (Figure 2A). The presence of phosphate did not affect the size or morphology of the nanoparticles. EDS of R5 templated TiO_2 particles confirmed the presence of titanium (Supporting Information). Samples synthesized in phosphate buffer displayed an additional phosphate emission line, indicating the association of phosphate with the nanoparticle. IR spectra of R5 templated TiO_2 nanoparticles synthesized in water and phosphate buffer revealed peptide amide stretching frequencies at 1649 and 1640 cm^{-1}, indicating the association of R5 peptide with the nanoparticles (Supporting Information).[36] The presence of the peptide frequencies in the IR spectroscopy, as well as the fact that only 20% of the starting material is consumed in the reaction, suggests that the peptide may be encapsulated in the forming nanoparticles.[37] Additionally, particles prepared in phosphate buffer showed a broad transition at 998 cm^{-1}, attributed to the P−O vibration similar to that observed in other metal oxides synthesized in the presence of phosphate ions.[38−41]

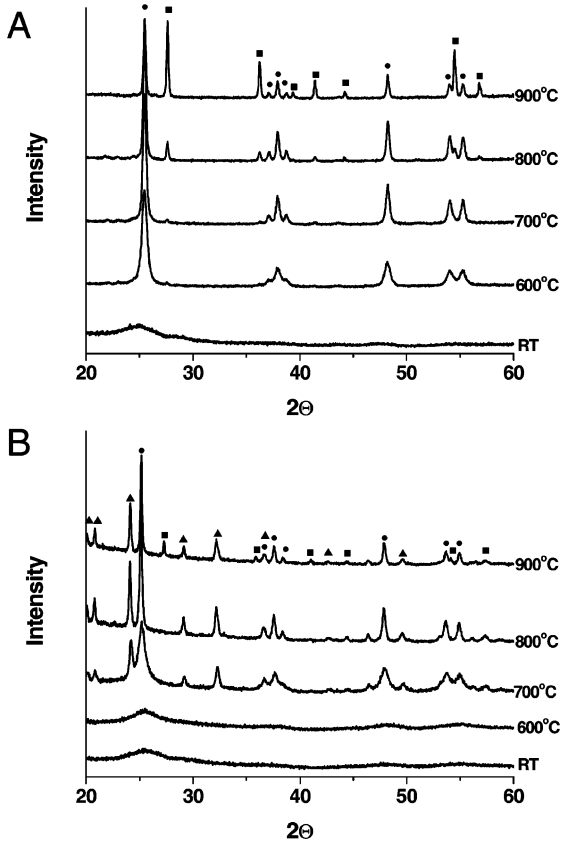

Figure 3. (A) Variable temperature XRD of R5 templated TiO_2 synthesized in water. (B) Variable temperature XRD of R5 templated TiO_2 synthesized in 100 mM phosphate buffer, pH 7.5 (●, anatase; ■, rutile; and ▲, titanium phosphate).

The nanoparticles formed in the presence of PLL displayed a Gaussian size distribution, with an average of approximately 140 $\pm$ 60 nm, according to SEM images (Figure 2B). In the case of PLL, it has been suggested that the secondary structure of the polymer can direct the morphology of the nanoparticles.[42,43] PLL with chain lengths ranging from 100 to 840 amino acids results in the formation of silica platelets, while silica nanospheres are formed from PLL with chain lengths under 100 amino acids.[42,43] Previously, CD studies have shown that in the presence of phosphate and silicic acid, PLL with a chain length above 100 amino acids adopts an α-helical structure, resulting in the formation of silica platlets.[42,43] In contrast, CD spectra of PLL with 266 amino acids in the presence of TBALDH showed little, if any, indication of secondary structure, consistent with the formation of spherical nanoparticles (Supporting Information). EDS of the nanoparticles confirmed the presence of titanium, as well as phosphate, if buffer was present (Supporting Information).

XRD. An XRD study of the phase transition in R5 and PLL templated TiO_2 synthesized in the absence and presence of phosphate was performed (Figures 3 and 4) with results summarized in Table 2. The transition from anatase to rutile

(33) van Bommel, K. J. C.; Jung, J. H.; Shinkai, S. *Adv. Mater.* **2001**, *13*, 1472−1476.
(34) Coradin, T.; Lopez, P. J. *ChemBioChem* **2003**, *4*, 251−259.
(35) Coradin, T.; Durupthy, O.; Livage, J. *Langmuir* **2002**, *18*, 2331−2336.
(36) Pretsch, E., Buhlmann, P., Affolter, C., Eds. *Structure Determination of Organic Compounds*; Springer: Berlin, 2000.
(37) Knecht, M. R.; Wright, D. W. *Langmuir* **2004**, *20*, 4728−4732.
(38) Conner, P. A.; McQuillan, A. J. *Langmuir* **1999**, *15*, 2916−2921.
(39) Yu, J. C.; Zhang, L.; Zheng, Z.; Zhao, J. *Chem. Mater.* **2003**, *15*, 2280−2286.
(40) Combes, C.; Rey, C.; Freche, M. *Colloids Surf., B* **1998**, *11*, 15−27.
(41) Isabel, T.-T. M.; Anderson, M. A. *Langmuir* **1990**, *6*, 602−611.
(42) Tomczak, M. M.; Glawe, D. D.; Drummy, L. F.; Lawrence, C. G.; Stone, M. O.; Perry, C. C.; Pochan, D. J.; Deming, T. J.; Naik, R. R. *J. Am. Chem. Soc.* **2005**, *127*, 12577−12582.
(43) Patwardhan, S. V.; Maheshwari, R.; Mukherjee, N.; Kiick, K. L.; Clarson, S. J. *Biomacromolecules* **2006**, *7*, 491−497.

Table 2. Scherrer's Analysis of R5 Peptide and PLL Templated TiO_2[a]

		water		phosphate buffer (100 mM, pH 7.5)		
peptide template	temperature	anatase size (nm)	rutile size (nm)	anatase size (nm)	rutile size (nm)	$Ti_4P_6O_{23}$ size (nm)
R5 peptide	25 °C	n/a	n/a	n/a	n/a	n/a
	600 °C	12.9 ± 2.5	n/a	2.58 ± 0.41	n/a	n/a
	700 °C	20.1 ± 1.4	n/a	10.8 ± 0.25	n/a	26.2 ± 0.55
	800 °C	29.7 ± 0.63	42.3 ± 0.89	28.6 ± 0.87	n/a	38.4 ± 1.2
	900 °C	37.3 ± 0.52	53.1 ± 0.74	31.1 ± 1.4	49.7 ± 2.3	43.0 ± 1.9
PLL	25 °C	n/a	n/a	n/a	n/a	n/a
	600 °C	14.7 ± 2.4	n/a	3.65 ± 0.72	n/a	n/a
	700 °C	26.5 ± 3.2	27.2 ± 2.23	17.4 ± 1.36	n/a	21.7 ± 2.3
	800 °C	28.6 ± 1.60	34.9 ± 1.82	17.6 ± 0.58	n/a	24.9 ± 0.87
	900 °C	n/a	36.1 ± 1.69	25.8 ± 1.52	67.9 ± 3.2	25.5 ± 1.5

[a] n/a indicates that no peak was present.

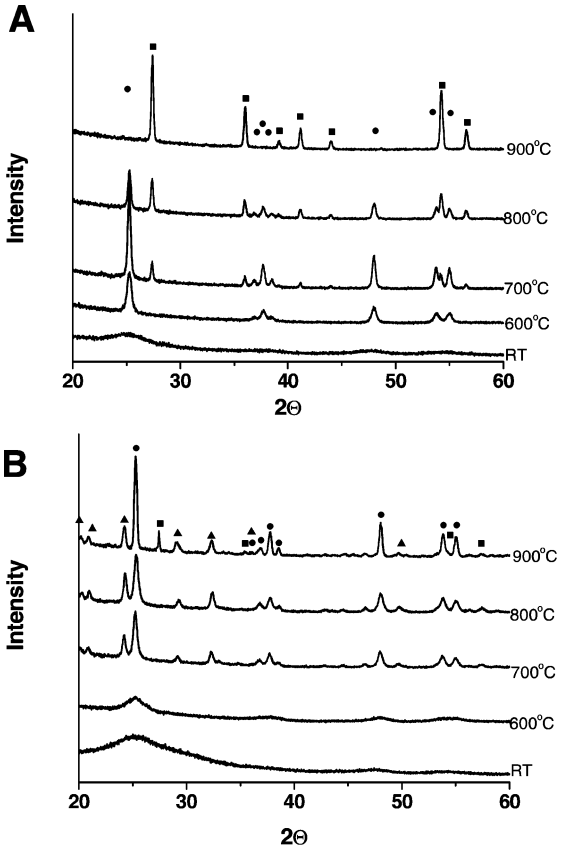

Figure 4. (A) Variable temperature XRD of PLL templated TiO_2 in water. (B) Variable temperature XRD of PLL templated TiO_2 synthesized in 100 mM phosphate buffer, pH 7.5 (●, anatase; ■, rutile; and ▲, titanium phosphate).

has been generally classified as an intermediate topotactic phase transition, with two Ti−O bonds breaking and reforming in the transition from distorted face centered cubic anatase to distorted hexagonal closest packed rutile.[44] Observed increases in crystallite sizes from anatase to rutile are consistent with the proposed mechanism of the TiO_2 phase transition. R5 templated TiO_2 synthesized *sans* phosphate buffer was amorphous at room temperature (Figure 3A). The crystalline anatase phase was observed at 600 °C. At 700 °C, the phase transition from anatase to rutile was evident. At 900 °C, approximately 50% of the anatase phase is converted to rutile. PLL templated TiO_2 was also poorly crystalline at room temperature (Figure 4A). Similar to R5 TiO_2, the anatase phase is present at 600 °C and the transition from anatase to rutile occurs at 700 °C. Unlike the R5 templated TiO_2, anatase to rutile phase conversion is complete at 900 °C. In contrast, for TiO_2 templated on protein fibers of silicatein, the anatase to rutile phase transition occurred at 825 °C, 125 °C higher than observed here.[10] This delay in transition temperature was previously attributed to the presence of carbon[45,46] from the silicatein filaments or the precursor. This seems unlikely, however, as the R5 template or PLL would also have similar amounts of carbon from constituent amino acids. A more likely explanation, as proposed by Morse et al., is that the strain energies imposed from the interacting template result in the delay of transition temperature, suggesting tighter interactions between the self-assembled peptide templates.[10]

The XRD variable temperature studies for PLL and R5 templated TiO_2 in phosphate buffer are remarkably similar. TiO_2 synthesized by either of the peptides in the presence of phosphate buffer is amorphous at room temperature (Figures 3B and 4B). Calcination of the sample revealed a crystalline anatase phase at 700 °C. Additionally, a small amount of titanium phosphate ($Ti_4P_6O_{23}$) is formed at 700 °C and higher temperatures. The formation of $Ti_4P_6O_{23}$ has been previously seen in deamination of $NH_4Ti_2P_3O_{12}$ at 770 °C.[47,48] Here, the release of NH_4^+ from degradation of the R5 peptide or NH_4^+ counterion present from the precursor could facilitate the formation of $Ti_4P_6O_{23}$. At 900 °C, there was a transition from anatase to rutile, an increase in transition temperature of some 200 °C. Phosphate that has been trapped, absorbed on the surface, or incorporated into the crystal lattice has been shown to inhibit movement of oxygen atoms necessary for the phase transition, thereby increasing the transition temperature.[49] Such a mechanism would be consistent with these experimental observations.

Conclusion

The often extreme conditions of metal oxide synthesis can be limiting when working with biological materials or constructing delicate nanodevices. Increasingly, biomimetic processing is being adapted for the synthesis of non-natural materials. For example, PLL has been used to form not only

(44) Shannon, R. D.; Pask, J. A. *Am. Mineral.* **1964**, *49*, 1707−1717.
(45) Hahn, H.; Logas, J.; Averback, R. S. *J. Mater. Res.* **1990**, *5*, 609−614.
(46) Gruy, F.; Pijolat, M. *J. Am. Ceram. Soc.* **1992**, *75*, 663−666.
(47) Ono, A. *J. Solid State Chem.* **1985**, *56*, 260−262.
(48) Horiuchi, S.; Ono, A. *J. Solid State Chem.* **1986**, *62*, 335−341.
(49) Criado, J.; Real, C. *J. Chem. Soc., Faraday Trans.* **1983**, *79*, 2765−2771.

silica but also germanium dioxide.[22] More recently, the R5 peptide has been used to form composite carbon nanotube/metal oxide structures.[26] Given that the proposed mechanism of silica formation by the R5 peptide is based on a combination of interactions that effectively concentrate the negatively charged silicate species at the peptide template primed to drive acid/base hydrolysis and condensation, the R5 peptide should be able to form alternative metal oxides as well. When the non-natural precursor TBALDH is used, the R5 peptide assembly readily formed TiO_2 nanoparticles under ambient conditions. Additionally, the interaction between the template and TiO_2 modulated the anatase to rutile phase conversion, resulting in generally lower transition temperatures than other biogenic TiO_2. Similar behavior was observed for the primary amine rich PLL template. The ability of the R5 peptide to form other non-natural metal oxides is currently under investigation.

Acknowledgment. The authors wish to thank the National Science Foundation (CMS-0508404) for support of this work.

Supporting Information Available: Titanium dioxide production as a function of R5 peptide concentration, titanium dioxide production as a function of pH, titanium dioxide production as a function of PLL concentration, CD of PLL in phosphate buffer, CD of PLL in the presence of phosphate buffer and TBALDH, CD of PLL in water, CD of PLL in water and TBALDH, EDS of R5 templated TiO_2 synthesized in the presence of phosphate buffer, EDS of R5 templated TiO_2 synthesized in the presence of water, EDS of PLL templated TiO_2 synthesized in the presence of water, EDS of PLL templated TiO_2 synthesized in the presence of phosphate buffer, IR of R5 peptide, IR of R5 templated TiO_2 synthesized in the presence of water, and IR of R5 templated TiO_2 synthesized in the presence of phosphate buffer. This material is available free of charge via the Internet at http://pubs.acs.org.

CM060342P